Biophysical Journal Volume 94 June 2008 4515–4524

Optical Lock-In Detection of FRET Using Synthetic and Genetically Encoded Optical Switches

Shu Mao,* Richard K. P. Benninger,† Yuling Yan,‡ Chutima Petchprayoon,* David Jackson,* Christopher J. Easley,† David W. Piston,† and Gerard Marriott*

*Department of Physiology, University of Wisconsin-Madison, Madison, Wisconsin; †Molecular Physiology and Biophysics, Vanderbilt University, Nashville, Tennessee; and ‡Department of Otolaryngology, Stanford University, Stanford, California

ABSTRACT The Förster resonance energy transfer (FRET) technique is widely used for studying protein interactions within live cells. The effectiveness and sensitivity of determining FRET, however, can be reduced by photobleaching, cross talk, autofluorescence, and unlabeled, endogenous proteins. We present a FRET imaging method using an optical switch probe, Nitrobenzospiropyran (NitroBIPS), which substantially improves the sensitivity of detection to <1% FRET efficiency. Through orthogonal optical control of the colorful merocyanine and colorless spiro states of the NitroBIPS acceptor, donor fluorescence can be measured both in the absence and presence of FRET in the same FRET pair in the same cell. A SNAP-tag approach is used to generate a green fluorescent protein-alkylguaninetransferase fusion protein (GFP-AGT) that is labeled with benzylguanine-NitroBIPS. In vivo imaging studies on this green fluorescent protein-alkylguaninetransferase (GFP-AGT) (NitroBIPS) complex, employing optical lock-in detection of FRET, allow unambiguous resolution of FRET efficiencies below 1%, equivalent to a few percent of donor-tagged proteins in complexes with acceptor-tagged proteins.

INTRODUCTION

The Förster resonance energy transfer (FRET) technique is widely used to study biomolecular dynamics and protein interactions in live cells (1–3). FRET is ideally suited for these studies, as it combines the high sensitivity and spatial resolution of fluorescence detection with the ease of introducing genetically encoded donor (D) and acceptor (A) probes to specific proteins or to biosensors to measure Ca^{2+} (4) or cAMP (5). Most live-cell FRET imaging studies involve measuring a change in the fluorescence of a donor, such as cyan fluorescent protein (CFP), or an increase in the sensitized emission of an acceptor, such as yellow fluorescent protein (YFP) (6–10). Since the chromophores within CFP and YFP lie deep within the protein matrix, they will be separated in a protein complex by at least the R_o for CFP and YFP (5.0 nm) (11), limiting the maximum FRET efficiency to <50%. The size and geometry of proteins fused to CFP and YFP can often further reduce FRET efficiency to <10% (8). A thorough discussion on the challenges of accurately measuring FRET using genetically encoded proteins can be found in Piston and Kremers (12). Other factors that undermine FRET imaging of protein interactions in live cells include the presence of endogenous proteins that decrease the probability of forming a D-A pair in a single complex and the thermodynamics of complex formation, which rarely allows all donor-tagged proteins to form a complex with acceptor-tagged proteins.

We describe an approach for the first absolute and high precision measurements of FRET efficiency on the same FRET pair within the same cell. This approach is based upon the use of an optical switch acceptor probe, NitroBIPS (Fig. 1 *a*), which undergoes rapid and reversible orthogonal, optically driven transitions between a strongly absorbing merocyanine (MC) state with excellent spectral overlap with green fluorescent protein (GFP) fluorescence, and a colorless spiro (SP) state (13). By incorporating NitroBIPS as an acceptor in a FRET pair with a donor such as GFP, optically driven transitions of the NitroBIPS acceptor can be used to modulate the efficiency of FRET in the complex. Modulation of FRET efficiency through control of an optical switch probe (photochromic FRET) was first demonstrated using a model fluorophore-optical switch molecule in solution (14–16). In studies detailed herein, however, we exploit the rapid (17), reversible, and deterministic changes in the visible extinction coefficient of the NitroBIPS probe by recording measurements of the donor fluorescence in the absence (SP) and presence (MC) of the acceptor in the same FRET pair and in the same cell, even in the presence of noncomplexed donors, donor-photobleaching, or a time-varying background. By employing a defined train of optical perturbations to control the SP and MC states of the acceptor probe, it is possible to modulate the fluorescence intensity of the donor probe (and the MC fluorescence) with the same waveform. The time-varying change in donor emission, obtained over many cycles of optical switching, can be analyzed using an approach that shares similarities with lock-in and phase-selective detection, and so we describe the approach as optical lock-in detection of FRET (OLID-FRET).

OLID-FRET, utilizing NitroBIPS, is a technique similar in concept to both photoactivation of the acceptor (18) (SP-to-MC

Submitted October 31, 2007, and accepted for publication January 22, 2008.

Shu Mao and Richard K. P. Benninger contributed equally to this work.

Address reprint requests to Gerard Marriott, Dept. of Physiology, University of Wisconsin-Madison, 1300 University Ave., Madison, WI 53705. E-mail: GM@physiology.wisc.edu.

Editor: Cristobal G. dos Remedios.

0006-3495/08/06/4515/10 $2.00

doi: 10.1529/biophysj.107.124859

transition) and photobleaching of the acceptor (2,19) (MC-to-SP transition), which can detect FRET between labeled proteins and is used as an indicator of complex formation in cells. However, these approaches involve excited-state reactions that generate damaging radicals, and so they require control experiments to rule out the possibility that the photoactivation or photobleaching reactions will destroy local protein activity or trigger a stress response in the cell. Furthermore, since these photochemical reactions are irreversible, they can only be used for a single determination of FRET in a given cell. Use of optical switches such as NitroBIPS, however, allows these reactions to be performed over many cycles with limited generation of photoproducts. The ability to optically control the acceptor probe between the SP and MC states provides a powerful and precise approach to lock in and carry out phase-selective detection of donor signals associated with the no-FRET (GFP-SP) and FRET (GFP-MC) conditions at any time, or for multiple determinations of FRET efficiency during an experiment. We show that this allows detection of small subpopulations of protein complexes undergoing FRET over a high background of non-complexed proteins, with sensitivity many times what is currently achievable using conventional techniques.

Finally, as part of this new OLID-FRET approach, we describe a method for the in vivo labeling of genetically encoded fusion proteins with optical switches. A benzylguanosine derivative of NitroBIPS (BG-PEG-NitroBIPS) is used as a suicide substrate for a variant of alkylguanosine transferase (AGT; SNAP-tag) (20–23). This labeling system is used to link NitroBIPS to a GFP-AGT fusion protein in living cells. The GFP-AGT(NitroBIPS) conjugate is used as a model system to demonstrate the possibility of repeatedly measuring FRET efficiencies down to $<1\%$ in living cells.

MATERIALS AND METHODS

Absorption spectra were recorded on a 1601PC instrument (Shimadzu, Kyoto, Japan). Fluorescence spectroscopy was performed on an SLM-AB2 (ThermoElectron, Waltham, MA). Spectroscopic analyses of optical switching within larger volume samples (~0.2–1.0 ml) were achieved by using either the 365-nm or 546-nm lines of a 100 W Hg-arc lamp (Zeiss, Oberkochen, Germany) selected with interference filters, and by irradiating with a hand-held-Hg-arc lamp.

BG-PEG-NitroBIPS

The synthesis of BG-PEG-NitroBIPS was achieved by coupling the succinimidyl ester of NitroBIPS with BG-PEG-NH_2 (Covalys, Witterswil, Switzerland) in dimethyl formamide with tetraethylammonium. The product was purified by using silica gel (5:1, Hex/EtOAc).

Cloning, transfection, gene expression, and protein purification

GFP-AGT (Covalys) was subcloned into both the pTrchisC (Invitrogen, Carlsbad, CA) and pCDNA (Invitrogen) vectors between the XhoI and *Hin*dIII restriction sites. The JM109 *Escherichia coli* strain was transformed with the GFP-AGT plasmid. The GFP-AGT protein was expressed and purified according to the handbook of Ni-NTA affinity chromatography (Qiagen, Hilden, Germany). Swiss 3T3 cells were grown on glass coverslips and transiently transfected with the GFP-AGT pCDNA plasmid DNA using Lipofectamine (Invitrogen) according to the manufacturer's protocol. Cells were imaged 24–32 h after transfection.

Proteins and protein labeling

Labeling of AGT fusion proteins with NitroBIPS

NitroBIPS-BG probes were covalently attached to AGT fusion proteins as follows: in vivo, AGT gene transfected cells were treated with medium containing 0.5 μM BG-NitroBIPS probe for 30 min, then washed in imaging medium (125 mM NaCl, 5.7 mM KCl, 2.5 mM $CaCl_2$, 1.2 mM $MgCl_2$, 10 mM HEPES, 2 mM glucose, 1% BSA, pH 7.4) for 45 min; in vitro, AGT fusion proteins and BG-NitroBIPS were combined in a ratio of 1:2 ~ 1:5 for 30 min in 50 mM Tris, pH 8.0, and then passed over a PD-6 or PD-10 column in the same buffer to remove any unbound BG-NitroBIPS probe.

F-Actin

G-actin in G-buffer (5 mM Tris, 0.2 mM $CaCl_2$, 0.2 mM ATP, pH 8) was labeled with N-alkylmaleimido-NitroBIPS (24), according to the methods of Sakata et al. (13). F-actin composed of unlabeled and NitroBIPS-labeled actin was prepared by adding KCl and $MgCl_2$ to 0.1 M and 2 mM, respectively, and filaments were stabilized by adding excess fluorescein isothiocyanate (FITC)-phalloidin (Sigma, St. Louis, MO). The preparation was left overnight on ice and centrifuged at 100,000 *g*. The pellet was resuspended in F-buffer (G-buffer plus 0.1 M KCl and 2 mM $MgCl_2$). The sample shown in Fig. 1 contained 0.5 ml 6.9 μM G-actin and was labeled to ~66% with 5-maleimide-NitroBIPS (13,24) and polymerized to form F-actin filaments with 35 μl 100 μM FITC-phalloidin (Sigma).

OLID-FRET using GFP-AGT(NitroBIPS)

Single- and two-photon (25,26) imaging was performed on an LSM510 microscope with a 40× 1.2 NA objective (Zeiss) incorporating a mode-locked titanium sapphire laser oscillator (Chameleon, Coherent, Santa Clara, CA). Optical control of FRET between GFP and the MC state of NitroBIPS in the GFP-AGT fusion protein was achieved using a series of optical manipulation and interrogations of the image field. This optical switching of the SP state to the MC state of NitroBIPS was realized using sequential scanning of the image field with 720 nm delivered from the titanium sapphire laser. MC-fluorescence generated by 720 nm excitation was collected through a 565–615 nm bandpass filter with infrared blocking. Optical switching of the MC state to the SP state was achieved by sequential scanning of the image field using the 543-nm line of the helium neon laser with MC state fluorescence collected through a 560-nm long-pass filter. GFP fluorescence was imaged by using excitation of the field with 488 nm argon ion laser and collecting the fluorescence emission through a 505-nm long-pass filter, and was conducted twice for each optical switching cycle, immediately after the final 543-nm scan (SP state, no FRET) and immediately after the final two-photon scan (MC state, FRET).

Imaging, in vitro samples

BG-NitroBIPS labeled GFP-AGT solution was immobilized onto a polydimethylsiloxane microwell to create a thin (1–3 μm) layer of construct that allowed for full optical switching of NitroBIPS within the two-photon excitation volume. OLID-FRET was performed on these samples by scanning the sample using two-photon excitation of SP (720 nm) to trigger the SP-to-MC transition and 543 nm to trigger the MC-to-SP transition. Excitation of the MC state led to either photochemistry to form the SP state or else a return

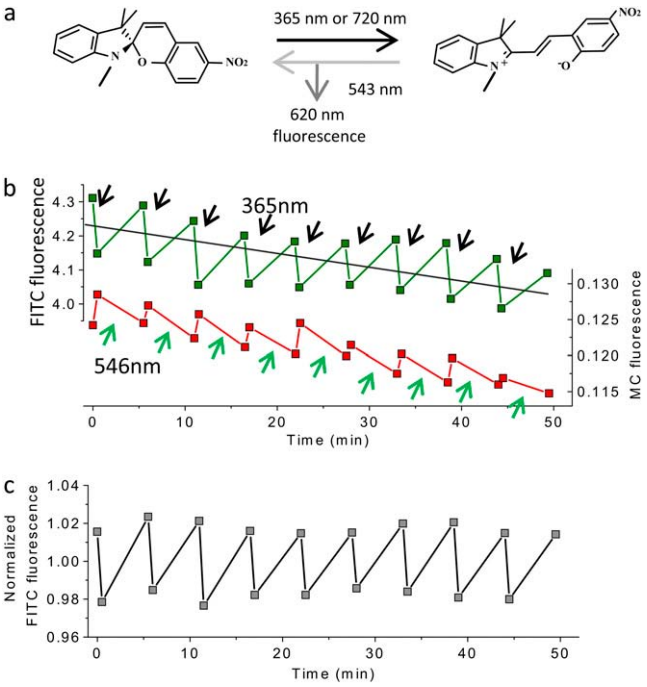

FIGURE 1 (*a*) Schematic representation of the optical transitions between the SP and MC states of NitroBIPS attached to a protein. Excitation of SP to MC occurs via one-photon excitation using 365 nm, or else by using two-photon scanning of an image field between 700 and 730 nm. Excitation of the MC state generates the MC excited state that decays either via photochemical transition to the SP state or by returning to the MC ground state with the emission of a red photon. Measurement of MC fluorescence in vitro or in vivo is used to determine the state of the switch, i.e., the amount of SP versus MC at any time and at any location in a cell. (*b*) Irradiation of a 1-ml sample of F-actin containing NitroBIPS-actin and FITC-phalloidin (Sigma) in F-buffer using the 365-nm output of a hand-held arc lamp for 30 s (*black arrows*) led to the conversion of SP to MC, whereas the MC state was converted back to SP by using a 5-min irradiation of the same sample with 546 nm light (*green arrows*). The change in FITC-phalloidin fluorescence in response to cycles of optical switching is shown in the green trace, whereas the corresponding red trace shows the change in the MC fluorescence of NitroBIPS-actin. High-fidelity reversible transitions between the MC and SP states on F-actin are shown for nine cycles of alternate irradiation of the sample in the cuvette with 365 nm and 546 nm light. (*c*) Normalizing FITC fluorescence reveals robust, uniform, and reversible optical switching of FRET that correlate with the periods of UV and 546-nm irradiation. The FRET efficiency for each cycle of optical-switching is uniform and generates an average value of 3.6 ± 0.4%.

to the MC ground state with the emission of a red photon. The MC fluorescence signal was used as a simple and sensitive readout of the state of the optical switch for both in vitro and in vivo imaging studies.

Imaging, in vivo samples

After labeling with BG-PEG-NitroBIPS, cells exhibiting a moderately strong GFP fluorescence were selected for study and were scanned sequentially with one switching cycle consisting of 1–10 720-nm scans followed by 10–20 543-nm scans. The cycle of optical switching between the SP and MC states and imaging of GFP fluorescence (see Fig. 4) was repeated up to 40 times. MC fluorescence recorded during two-photon and 543-nm scanning of the image field was used to show that transitions between the SP and MC states were complete and reversible. GFP fluorescence can decrease slowly during the course of an optical switching study due to photobleaching and sample drift, which otherwise undermines multiple determinations of FRET within long-term imaging studies. The advantage of the OLID of FRET described in this study is that the no-FRET condition is determined at the beginning of each optical-switch cycle throughout the course of the imaging study. These determinations serve to recalibrate the system for time-dependent changes in GFP fluorescence such as photobleaching or sample movement that would otherwise compromise the determination of FRET efficiency.

Data analysis

To determine the efficiency of energy transfer (E_T), the time-dependent GFP (donor) intensity is averaged over a region of interest in the cell or sample. Using a polynomial expansion, the intensity of GFP fluorescence is fit over the entire course of the optical switching study to provide a qualitative assessment of data correlation between the SP and MC states. The data set can furthermore be subject to a Fourier filter (see Fig. S1 in Supplementary Material, Data S1), which better reveals variations in the GFP intensity in the no-FRET (SP) and FRET (MC) states by removing all contributions that are out of phase and frequency with the optical switching, i.e., the ''DC'' and slowly varying components. FRET efficiency is determined for each cycle of optical switching by measuring the intensity of GFP fluorescence immediately before the first two-photon scan, which represents the SP state of the switch and the no-FRET condition, and immediately after the final two-photon scan, which represents the MC state and the FRET condition. The effective FRET efficiency, as used in Erickson et al. (8), is calculated using Eq. 1:

$$E_T = \frac{1}{n}\sum_{\text{cycles}} 1 - \frac{F_{DA}}{F_D}, \tag{1}$$

where F_D is the GFP intensity when the NitroBIPS is in the SP state (i.e., no-FRET condition), F_{DA} is the GFP intensity when NitroBIPS is in the MC state (i.e., FRET condition) and ''cycles'' refers to a summation over all switching cycles. Unless otherwise stated, the E_T is averaged over 10 switching cycles and across the number of separate sample preparations that is stated in the text. The error quoted in the mean E_T is the standard error of the mean, where n is the number of samples.

The Förster transfer distance R_0 is calculated by Eq. 2:

$$R_0^6 = \frac{9000(\ln 10)\phi_D\kappa^2}{128\pi^5 N n^4} J(\lambda), \tag{2}$$

where ϕ_D is the quantum yield of the donor in the absence of acceptor (for EGFP, $\phi_D = 0.60$); n is the refractive index of the medium (for water, $n = 1.35$); κ^2 is a factor describing the relative orientation in space between the transition dipole moments of the donor and acceptor, usually assumed to be 2/3; $J(\lambda)$ is the overlap integral, which expresses the degree of spectral overlap between the donor emission and the acceptor absorption (for EGFP and NitroBIPS, $J(\lambda) = 8.817 \times 10^{14}$). R_0 is thus calculated to be 46 Å (4.6 nm).

The distance between the donor and acceptor (R) can then be calculated from E_T and the Förster transfer distance R_0 by using Eq. 3:

$$R = R_0 \times \sqrt[1/6]{\left(\frac{1}{E_T} - 1\right)}, \tag{3}$$

where $R_0 = 4.6$ nm.

RESULTS AND DISCUSSION

Optical switching of NitroBIPS

NitroBIPS undergoes rapid, reversible, and efficient orthogonal optically driven transitions between the SP and MC states (Fig. 1 *a*) without significant fatigue (13,15,16,24). The

extinction coefficient of the ~500–600 nm absorption of NitroBIPS changes from almost zero in SP to 51,000 M^{-1} cm^{-1} in MC (24) (Fig. 2, *c* and *d*). Excitation of SP using 365 nm (ultraviolet (UV)) excitation, or as shown in this study by using two-photon excitation, which causes less phototoxicity, converts SP to MC within microseconds. The MC-to-SP transition is triggered by excitation of MC with 543 nm although the MC excited state can decay back to the MC ground state with red fluorescence (~620 nm) (13). This emission provides a sensitive and convenient signal to image the optical switch and to monitor the efficiency of optical switching in cells.

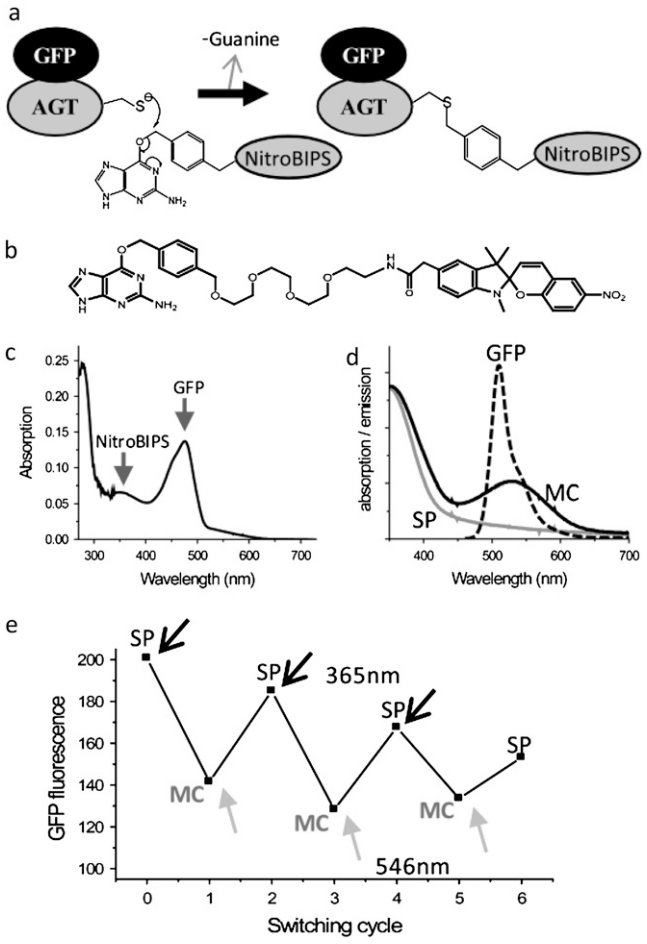

FIGURE 2 (*a*) Schematic representation of the in vitro and in vivo labeling of a GFP-AGT fusion protein with an optical switch modified from Kindermann et al. (20). The active-site cysteine residue on AGT attacks the benzylic carbon on the BG-PEG-NitroBIPS (*b*) substrate, forming a covalent linkage of the NitroBIPS probe with the thiol residue. (*c*) The reaction proceeds quantitatively in vitro, as determined by absorption spectroscopy of the SP state of the purified labeled fusion protein GFP-AGT (NitroBIPS). (*d*) The strong overlap between the GFP fluorescence emission spectrum (*dashed line*) and the NitroBIPS MC state absorption spectrum (*solid line*) leads to a high-energy transfer efficiency between GFP and MC-NitroBIPS. The subsequent optically driven transition of NitroBIPS to the SP state leads to a low overlap between the GFP fluorescence emission spectrum and the NitroBIPS SP state absorption spectrum (*gray line*), resulting in a poor energy-transfer efficiency. (*e*) The GFP fluorescence change of GFP-AGT(NitroBIPS) in response to 1 min irradiation with 365 nm UV, which increases the MC absorption and leads to FRET with a concomitant decrease in GFP emission. Contrariwise, irradiation of the MC state of the fusion protein for 1 min with 543 nm decreases the MC absorption, which decreases FRET and increases GFP emission. The frequency of the decreases and increases in donor emission correlate with the frequency and phase of UV and VIS pulses.

The principle of OLID-FRET was demonstrated using a preparation of F-actin in which FITC-phalloidin served as the donor and NitroBIPS-labeled actin as an optically switchable acceptor. The UV-driven SP-to-MC transition was monitored by recording the change in MC fluorescence (Fig. 1 *b*). Subsequent irradiation of the MC actin with 546 nm converted MC to SP with a concomitant decrease in MC fluorescence. As shown in Fig. 1 *b*, orthogonal optical switching of the SP and MC states led to a defined and reversible change in FITC intensity that correlates with the no-FRET (SP) and FRET (MC) states. This cycle of optical switching between the SP and MC states on the filaments was repeated nine times. The progressive decrease in FITC emission apparent in Fig. 1 *b* is due to photobleaching, which would usually lead to an overestimation of FRET efficiency and thereby undermine multiple determinations of FRET efficiency. However, the ability to optically generate the donor-only state (SP) via the MC-to-SP transition provides an effective method to measure the donor-only reference signal at any time, even with significant photobleaching. The value of FRET efficiency was similar over nine optical switching cycles and generated an average value of 3.6 ± 0.4% (Fig. 1 *c*).

A genetically encoded system for OLID-FRET

Having demonstrated the principle of OLID-FRET using synthetic donor and acceptor probes, we next asked whether similar FRET pairs could be generated using genetically encoded systems. The approach used to introduce NitroBIPS to a GFP-AGT fusion protein is summarized in Fig. 2 *a*. BG-PEG-NitroBIPS (Fig. 2 *b*) acts as a suicide substrate for AGT and exhibits a remarkable specificity for the transferase both in vitro and in vivo (20). Purified GFP-AGT provided a robust approach to quantify the efficiency and kinetics of NitroBIPS labeling and to characterize the optical-switch properties. Absorption spectroscopy showed that GFP-AGT was fully labeled with BG-PEG-NitroBIPS (Fig. 2 *c*). As expected, sequential irradiation of GFP-AGT(NitroBIPS) with 365 nm and 546 nm led to reversible and complete conversion between the SP and MC states with concomitant reversible modulation of GFP fluorescence (Fig. 2 *d*).

Purified GFP-AGT(NitroBIPS) was also used to study the properties and limits of detection using microscope-based OLID-FRET. FRET efficiencies were determined for defined mixtures of GFP-AGT(NitroBIPS) and the control protein, GFP-AGT, which cannot engage in FRET, using the optical switching protocol detailed in experimental methods. Fig. 3, *a* and *b*, displays the reversible optical switching of

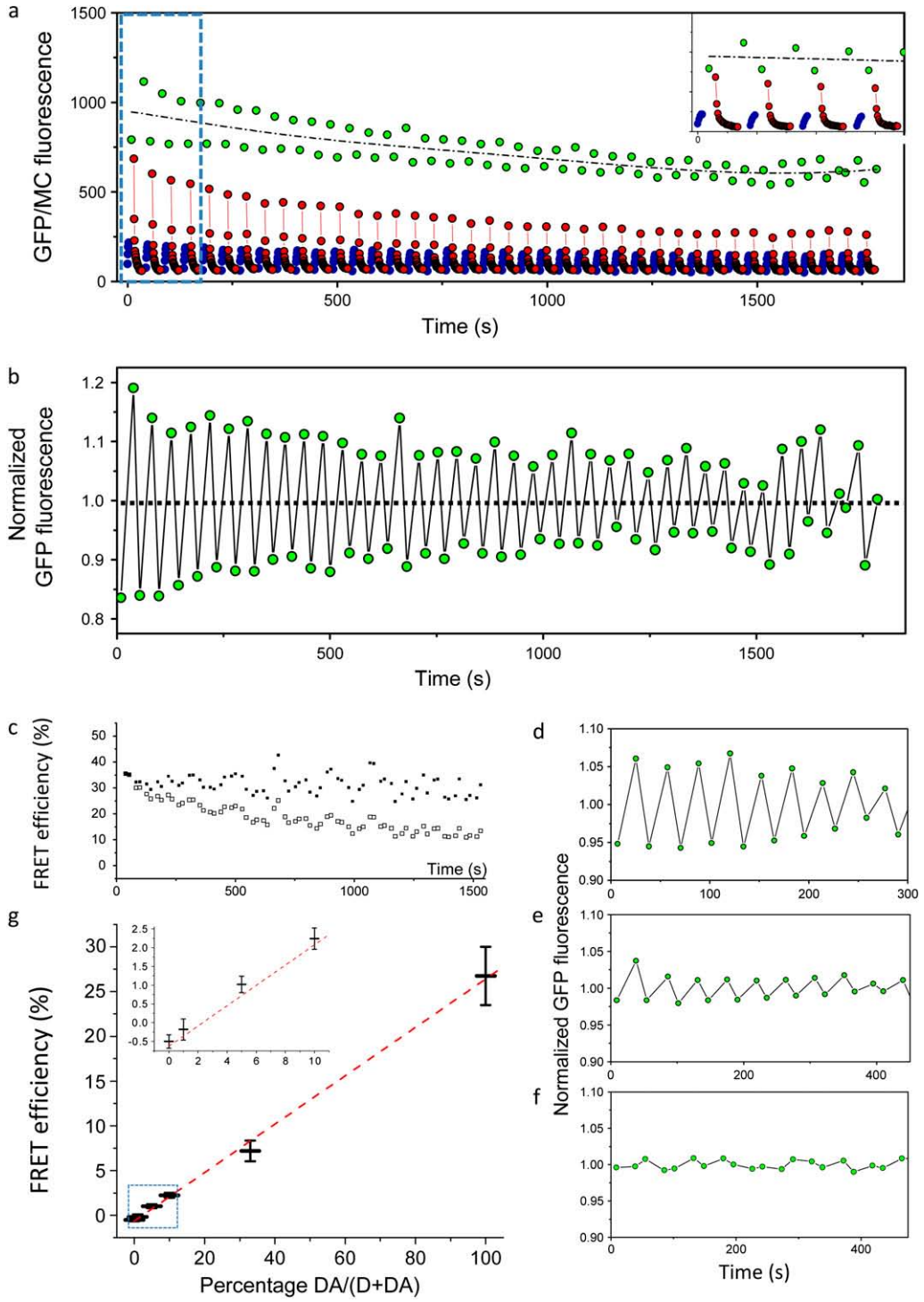

FIGURE 3 Microscope-based in vitro measurement of FRET in GFP-AGT(NitroBIPS). (*a*) Representative data of 100% labeled GFP-AGT(NitroBIPS) exhibiting reversible optical switching of MC fluorescence (*blue circles*, 720-nm two-photon excitation; *red circles*, 543-nm excitation) and GFP fluorescence (*green circles*). The optical transition between the MC and SP states continues to completion through visualizing MC fluorescence, with a switching efficiency of >90% (*inset*). Continual optical switching over an ~30-min period reduces GFP fluorescence by ~20% due to photobleaching, as shown by the GFP intensity trend (*black dash-dotted line*). (*b*) Normalizing GFP fluorescence by the trend accounts for removed photobleaching artifacts and clearly shows reversible donor optical switching due to FRET, as evidenced by modulation of GFP florescence in phase with optical perturbation of the NitroBIPS probe. (*c*) FRET efficiency calculated from donor intensity as a function of time (*open squares*). Over ~30 min of continuous optical switching, FRET efficiency is reduced by ~50% due to photobleaching of the NitroBIPS acceptor, as seen in *a*. Correcting for photobleaching of the NitroBIPS acceptor yields a constant FRET efficiency (*solid squares*). (*d*) Resultant normalized donor GFP modulation due to NitroBIPS optical switching in a mixture of 33% GFP-AGT(NitroBIPS)/67% unlabeled AGT-GFP. (*e*) The same as in *d*, but for a mixture of 10% GFP-AGT(NitroBIPS)/90% unlabeled AGT-GFP. (*f*) Resultant

GFP-AGT(NitroBIPS), as visualized through the GFP fluorescence over a 30-min period. For the GFP-AGT(NitroBIPS) complex, we measure a mean FRET efficiency of 26.7 ± 3.3% (Fig. 3 *g*). Since the R_0 for GFP and MC was calculated as 4.6 nm, the distance between the GFP and MC, assuming 100% labeling in the GFP-AGT fusion, is 5.5 nm and suggests that MC is located on the far side of GFP in the fusion protein. Due to continual irradiation over the 30-min experiment the GFP intensity decreases by ~20% due to photobleaching, whereas the peak MC fluorescence decreases by ~50%, following through to an ~50% decrease in FRET efficiency (Fig. 3 *c*). Normalizing the FRET efficiency to the acceptor MC fluorescence can correct for this reduction, also seen in Fig. 3 *c*. Although the optically driven switching of MC-to-SP is very efficient, the low probability of MC fluorescence (represented by ~3% quantum yield) can lead to permanent photobleaching. This photobleaching could be reduced by utilizing NitroBIPS derivatives having a lower quantum yield, or even a probe such as naphthozaxine, which switches with ~100% efficiency and has no fluorescence (13,24).

Due to the ability to repetitively turn on and off the visible absorption of the FRET acceptor, we can employ OLID microscopy to resolve fluctuations in the GFP intensity that correlate with the phase and frequency of optical perturbations. This should allow more sensitive detection of the FRET efficiency. To demonstrate this, we imaged FRET in samples of GFP-AGT where a known proportion of the GFPs are undergoing FRET with a NitroBIPS (MC) acceptor, with the rest of the GFPs having no acceptor and acting as a non-FRET background. This is similar to performing a FRET experiment where only a subpopulation of the protein under study forms a complex, which generally limits the use of FRET (see Introduction). Fig. 3 *d* displays GFP fluctuation data from samples where the ratio of GFP-AGT(NitroBIPS) to GFP is 1:2, and Fig. 3 *e* displays the results using a stoichiometry of 1:10, where modulation of the donor fluorescence in phase with the acceptor switching is still clearly observed.

From imaging samples containing 100% control GFP (Fig. 3 *f*), we observed a random uncorrelated GFP intensity. Nevertheless, an apparent FRET efficiency of −0.5 ± 0.2% ($n = 10$ samples) is observed when data is averaged over multiple switching cycles. We attribute this to slight instabilities in the microscope when switching between excitation configurations, although it is possible that the GFP probe like Dronpa (27) may exhibit a small amount of optical switching. These intensity fluctuations are also observed when the switching cycles are performed with 0 mW excitation for the SP-to-MC and MC-to-SP transitions, but not when imaging GFP without any switching cycles (data not shown). In Fig. 3 *g*, the calculated FRET efficiency is shown for a number of FRET-pair dilutions, revealing a linear relationship between the FRET efficiency averaged over 10 switching cycles and the proportion of FRET complexes. For example, the sample containing 100% GFP-AGT(NitroBIPS) in the MC state has a mean FRET efficiency of 26.7 ± 3.3% ($n = 5$ samples), whereas the sample with a mixture of 10% GFP-AGT(NitroBIPS)/90% GFP has a mean FRET efficiency of 2.2 ± 0.3% ($n = 7$ samples). When imaging <5% GFP-AGT(NitroBIPS)/95% GFP, random uncorrelated fluctuations (similar to that seen in Fig. 3 *f*) dominate the GFP signal. Nevertheless, through OLID, the mean FRET efficiency for 5% GFP-NitroBIPS(MC)/95% GFP, averaged over 10 cycles, was found to be 1.3 ± 0.1% ($n = 6$ samples). This is significantly above the measurement for 0% GFP-NitroBIPS(MC) ($P = 5.3 \times 10^{-5}$, Student's *t*-test), such that although random fluctuations can mask individual switching cycles in the donor intensity, OLID allows the resolution of the GFP donor signal that is locked in and in phase with the train of optical perturbations that control NitroBIPS. Thus, OLID-FRET can be used to resolve protein complexes in samples containing ~3% GFP-NitroBIPS in the presence of a 97% GFP background, with only the uncorrelated intensity fluctuations limiting the significant detection of smaller subpopulations.

Optical-switching of FRET in fusion proteins in living cells

Defined sequences of optical perturbation and GFP imaging of the GFP-AGT(NitroBIPS) FRET pair was used to demonstrate the principles and practice of OLID-FRET in cells. The delivery of NitroBIPS to specific proteins was achieved by using the AGT (SNAP-tag) labeling approach (20–23). Several probes were prepared by coupling the succinimidyl ester of 4-NitroBIPS to amine-terminated benzyl guanosine derivatives (Covalys). These probes were added to the medium of Swiss-3T3 cells expressing the same GFP-AGT fusion protein described above. The in vivo reaction was optimized to increase the specificity of labeling and to prevent accumulation of the probe in vesicles and organelles. Previous unpublished studies (K. Johnsson) identified the SNAP-26 mutant of AGT as the best variant for in vivo labeling with BG-PEG-NitroBIPS. Although BG-PEG-NitroBIPS has a lower membrane permeability compared to probes with a shorter-linkage group, it was preferred because of the superior FRET efficiency, E_T, of 30 ± 5% vs. 15 ± 1% for BG-NitroBIPS (not shown). The distribution of MC fluorescence in labeled cells was uniform (Fig. 4 *c*).

FIGURE 3 (Continued).
donor fluctuations in 100% unlabeled AGT-GFP. (*g*) Calculated mean FRET efficiency (mean ± SE) for various dilutions of GFP-AGT(NitroBIPS) in unlabeled AGT-GFP. A linear relationship is found within experimental error. Dilutions down to <5% GFP-AGT(NitroBIPS) can be resolved and proven to be significant ($p = 5.3 \times 10^{-5}$, Student's *t*-test (see *inset*)).

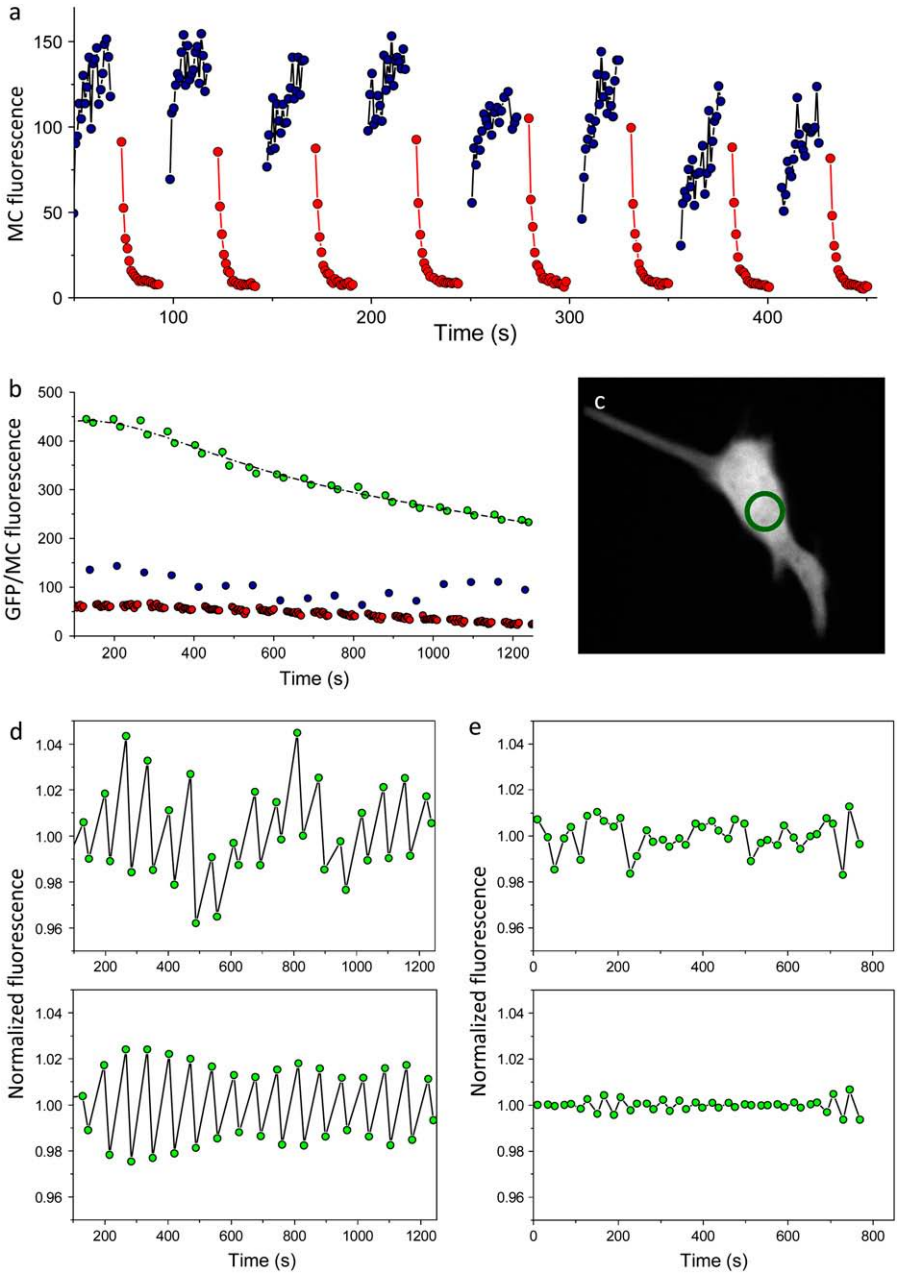

FIGURE 4 Microscope-based in vivo measurement of FRET in GFP-AGT(NitroBIPS). (*a*) Intensity of MC fluorescence recorded in a NitroBIPS-stained cell during the 720-nm (*blue*) and 543-nm (*red*) scanning periods of sequential optical-switch cycles. (*b* and *c*) Graphic representation of GFP fluorescence measurements (*b*) in a region of interest in a cell (*c*, *green circle*) for the SP and MC states. The GFP intensity is higher in the SP state (*blue circles*) compared to the MC state (*red circles*) for every pair of GFP measurements made through the optical switching experiment (17 cycles). The decrease in GFP intensity is due to focal drift and can be corrected for by normalizing to a trend (*black dashed line*). (*d*) Normalized GFP fluorescence from the GFP-AGT(NitroBIPS)-labeled cell shown in *b* and *c*. Reversible optical switching of donor GFP fluorescence is in phase with NitroBIPS acceptor optical switching, allowing an absolute measurement of the FRET efficiency in the living cell, in this case 3.3 ± 0.4% (*upper*). Fluctuations in the GFP signal that are not at the frequency and phase of the optical switching of FRET can be removed using a Fourier filter, giving a more precise measurement of the FRET efficiency of 3.3 ± 0.2% (*lower*). (*e*) Corresponding measurements of normalized GFP fluorescence in the unlabeled AGT-GFP-expressing cell, before (*upper*) and after (*lower*) performing a Fourier filter. The absence of a NitroBIPS acceptor does not lead to any correlation between the donor fluorescence and the phase of optical perturbations of the cell using 720 nm and 543 nm lasers.

A single optical switch cycle involved the following operations: 1), scan the image field 10–20 times at 543 nm to convert all of the MC to SP; 2), scan the field with a single scan at 488 nm and record GFP emission at 520 nm, which provides a reference signal for the no-FRET condition; 3), scan the field with 1–10 scans at 720 nm (two-photon irradiation) to completely convert SP to MC, the number of scans required to quantitatively convert the SP to MC depending on the laser power and tolerance of the cell to two-photon irradiation; 4), scan the image at 488 nm and record the GFP emission—the GFP intensity within this image data represents the FRET condition and is compared with the GFP intensity in the preceding reference scan. The cycle is repeated by scanning the image field 10–20 times with 543 nm to convert MC to SP (step 1). This cycle is repeated numerous times, and 17 cycles were used for the study represented in Fig. 4 *b*.

As shown in Fig. 4, *a* and *b*, two-photon (720-nm) scanning of the image field led to the formation of the MC state of GFP-AGT(NitroBIPS) and was accompanied by an increase in MC fluorescence and a decrease in GFP fluorescence as a result of FRET. Orthogonal manipulation of the MC state in the fusion protein by scanning the field at 543 nm formed the SP state of GFP-AGT(NitroBIPS) and relieved FRET, as seen by the decrease in MC fluorescence and increase in GFP fluorescence. The percentage change in the GFP intensity

between the SP and MC states does not alter upon a longer exposure of the cell to 720 nm or 543 nm, suggesting that the transitions for all molecules in the interrogated volume are complete (Fig. 4 *a*).

The progressive decrease in GFP fluorescence (Fig. 4 *b*) is a result of cell movement and drift, as well as some photobleaching due to direct excitation of GFP with 488 nm and to a lesser extent by two-photon excitation. A GFP-intensity trend is thus fit to the data (Fig. 4 *d*). A further limitation of conventional FRET imaging studies is that FRET efficiency measured by the decrease in donor emission cannot be conducted within the same cell. These problems, which limit the usefulness of conventional FRET imaging approaches, can be overcome using OLID-FRET. Thus, by updating the measurement of GFP intensity in the SP state within each optical-switch cycle, it is possible to make a new and accurate determination of FRET efficiency even when only a few percent of donor probes engage in FRET (Fig. 4 *d*). Despite this condition, the values of FRET efficiency determined over the 33 optical-switch cycles are uniform and highly correlated. (We note that very low photobleaching was generally observed when imaging OLID-FRET in live cells, as seen in Fig. S2 in Data S1, which shows no sample movement or focal drift). Control experiments using the optical-switch protocol, as described in Fig. 4 *b*, were conducted for cells without BG-PEG-NitroBIPS. As expected, the corresponding measurement of GFP fluorescence after the two-photon and 543-nm scans exhibited no periodic switching (Fig. 4 *e*). Despite this lack of correlated switching, the residual fluctuation averaged out to an apparent FRET efficiency between -0.5% and $+0.5\%$, as also seen in the in vitro measurements in Fig. 3.

The small change in GFP signal between the SP and MC states of the acceptor in cells, as compared with in vitro data, suggest that only a small fraction of AGT was labeled within the cell. Based on the in vitro data in Fig. 3 *g*, the $4.0 \pm 0.5\%$ average change in GFP signal between the SP and MC states corresponds to $\sim$20% labeling efficiency. Further, in vivo measurements of FRET efficiency as low as $0.97 \pm 0.09\%$ have been measured for GFP-AGT(NitroBIPS) (data not shown), demonstrating that through application of OLID-FRET we can reliably detect GFP-AGT when only 4% of the acceptor is labeled to AGT. The highest measured FRET efficiency of GFP-AGT(NitroBIPS) in vivo was $7.8 \pm 1.8\%$, representing a labeling ratio of BG-PEG-NitroBIPS to GFP-AGT of $\sim$31%. We speculate that the poor efficiency of BG-PEG-NitroBIPS labeling to the fusion protein results from its limited membrane permeability, which should be improved on using a less polar linker between BG and NitroBIPS (S. Mao, unpublished results). Despite the low in vivo labeling of AGT-GFP with BG-PEG-NitroBIPS, OLID-FRET provides accurate, reproducible, and multiple measurements of FRET between specific proteins in living cells over a long-term imaging study. The ability to measure $<1\%$ FRET efficiencies when $<5\%$ of the donor probe is undergoing FRET with an acceptor probe will be powerful in resolving subpopulations of interaction species in live cells. Through application of OLID-FRET with the genetically targeted GFP-NitroBIPS construct, we can readily achieve sensitivities in live cells far superior to those found using conventional FRET techniques.

The three-cube method for imaging FRET efficiency requires intensity measurements in reference samples that are sensitive to photobleaching and instrumentation effects, although careful studies by Yue and co-workers led to reliable single-time-point measurements down to a few percent (8,9). However, absolute determination of FRET efficiency in live cells remains a formidable challenge. Some studies have proposed corrections, relying on procedures such as gradual donor and acceptor photobleaching (28), or intensity imaging in multiple-reference FRET constructs (29), and measuring absolute FRET efficiency of $>10\%$. A correction utilizing lifetime measurements of FRET systems with known stoichiometry (30) enabled determination of FRET in the presence of 90% free donor, although complications due to photobleaching were not accounted for. However, many of these techniques require multiple reference measurements to be made to remove any ambiguity as to whether FRET is occurring. Furthermore, a quantitative comparison of methods concluded that resolving stoichiometires of $<1{:}10$ was unreliable (31). Sophisticated techniques for imaging FRET have been successfully employed to resolve FRET efficiencies more directly (i.e., through the use of fewer reference measurements) down to $E \approx 5\%$, including polarization-resolved fluorescence imaging (32) and fluorescence lifetime imaging (33). Using OLID-FRET, however, we can unambiguously and uniquely detect FRET efficiencies of $<1\%$ in a single cell measurement to resolve small subpopulations of species undergoing FRET in the presence of 95% free donor. The limiting factor in resolving smaller FRET efficiencies is to be able to filter out random uncorrelated donor fluorescence fluctuations, which in our case start to dominate the FRET-modulated donor signal at $\sim$1% energy transfer efficiency. As discussed in Fig. S1 in Data S1, imaging a greater number of switching cycles allows a greater degree of filtering of uncorrelated fluctuations, thus improving sensitivity. In this study, we are limited to a cycle time of $\sim$25–50 s, which includes a significant amount of instrument dead time ($\sim$15 s/cycle). However, FRET efficiency measurements can be accelerated by reducing the field of view or by using faster line-scan excitation, for example, on the Zeiss Five-Live microscope. Since FRET efficiency can often be determined with sufficient accuracy using only two measurements of the donor emission (i.e., the pre- and post-two-photon pulse), it allows for multiple and rapid measurements of FRET efficiency in a single cell, which is an invaluable feature for long-term studies in which donor probes undergo photobleaching, and in situations where there are spatiotemporal variations in background signal.

Optical switching of FRET efficiency was first demonstrated for a model fluorophore-switch molecule in solution by Erijman and colleagues (14) (photochromic-FRET). Other studies (15,16) have reported that optical control of the SP and MC states of NitroBIPS linked to Qdots could be used to modulate the intensity of the fluorescent nanoparticle. However, the FRET efficiency measured in these systems exhibited unusual dependence on the number of acceptor molecules (up to 100) on each Qdot (15), or on proximity (34). Regardless, none of these studies detailed approaches such as those shown herein for specific labeling of optical switches to proteins in live cells, and for imaging and analysis of the modulated FRET signal within these genetically encoded proteins for multiple determinations of FRET efficiency under conditions where only a small percentage of protein-labeled donor probe engages in FRET with the optical-switch acceptor-labeled protein.

Using more photostable optical switch probes with lower fluorescence quantum yields will allow more rapid switching. Together with optimized instrument stability, we envisage more rapid measurements of FRET, enabling the detection of transfer efficiencies $<0.1\%$, equivalent to $<1\%$ of donors engaging in FRET. Further improvements to OLID-FRET include the generation of all genetically encoded probes. In particular, the GFP-related optical switch Dronpa (27), like NitroBIPS, undergoes rapid and reversible excited-state transitions between a nonfluorescent *cis* state and a fluorescent *trans* state that exhibit high extinction at 503 nm. Thus, we anticipate that OLID-FRET-based imaging of protein interactions should also be possible using a BFP- or CFP-Dronpa FRET pair, whereas more optimized systems for live-cell imaging will no doubt emerge with the development of red-shifted mutants of Dronpa.

Thus, we show that OLID-FRET is a powerful technique for dynamically mapping very low FRET efficiencies in live cells, particularly when trying to resolve small subpopulations of binding species against a high and time-varying background of nonbinding species, a common occurrence in biological phenomena.

SUPPLEMENTARY MATERIAL

To view all of the supplemental files associated with this article, visit www.biophysj.org.

This project was supported by grants to G.M. from the National Institutes of Health (R01EB005217), DARPA-SPARTAN (19182-S2), and the Human Frontiers Science Program Organisation (RGP0045), and by grants to D.W.P. from the National Institutes of Health (R01-DK53434 and P20-GM72048) and the Medical Free-Electron Laser Program.

REFERENCES

1. Yan, Y., and G. Marriott. 2003. Analysis of protein interactions using fluorescence technologies. *Curr. Opin. Chem. Biol.* 7:1–6.
2. Jares-Erijman, E., and T. Jovin. 2003. FRET imaging. *Nat. Biotechnol.* 21:1387–1395.
3. Koyama-Honda, I., K. Ritchie, T. Fujiwara, R. Iino, H. Murakoshi, R. S. Kasai, and A. Kusumi. 2005. Fluorescence imaging for monitoring the colocalization of two single molecules in living cells. *Biophys. J.* 88:2126–2136.
4. Miyawaki, A., J. Llopis, R. Heim, J. M. McCaffery, J. A. Adams, M. Ikura, and R. Y. Tsien. 1997. Fluorescent indicators for Ca^{2+} based on green fluorescent proteins and calmodulin. *Nature.* 388:882–887.
5. Nagai, Y., M. Miyazaki, R. Aoki, T. Zama, S. Inouye, K. Hirose, M. Iino, and M. Hagiwara. 2000. A fluorescent indicator for visualizing cAMP-induced phosphorylation in vivo. *Nat. Biotechnol.* 18: 313–316.
6. Rizzo, M. A., G. H. Springer, B. Granada, and D. W. Piston. 2004. An improved cyan fluorescent protein variant useful for FRET. *Nat. Biotechnol.* 22:445–449.
7. Nagai, T., K. Ibata, E. S. Park, M. Kubota, K. Mikoshiba, and A. Miyawaki. 2002. A variant of yellow fluorescent protein with fast and efficient maturation for cell-biological applications. *Nat. Biotechnol.* 20:87–90.
8. Erickson, M., B. A. Alseikhan, B. Z. Peterson, and D. T. Yue. 2001. Preassociation of calmodulin with voltage-gated Ca^{2+} channels revealed by FRET in single living cells. *Neuron.* 31:973–985.
9. Erickson, M.,. H. Liang, M. X. Mori, and D. T. Yue. 2003. FRET two-hybrid mapping reveals function and location of L-type Ca^{2+} channel CaM preassociation. *Neuron.* 39:97–107.
10. Vanderklish, P. W., L. A. Krushel, B. H. Holst, J. A. Gally, K. L. Crossin, and G. M. Edelman. 2000. Marking synaptic activity in dendritic spines with a calpain substrate exhibiting fluorescence resonance energy transfer. *Proc. Natl. Acad. Sci. USA.* 97:2253–2258.
11. Patterson, G., D. Piston, and B. Barisas. 2000. Forster distances between green fluorescent protein pairs. *Anal. Biochem.* 284:438–440.
12. Piston, D. W., and G. J. Kremers. 2007. Fluorescent protein FRET: the good, the bad and the ugly. *Trends Biochem. Sci.* 32:407–414.
13. Sakata, T., Y. Yan, and G. Marriott. 2005. Optical-switching of dipolar interactions on proteins. *Proc. Natl. Acad. Sci. USA.* 102:4759–4764.
14. Giordano, L., T. M. Jovin, M. Irie, and E. A. Jares-Erijman. 2002. Diheteroarylethenes as thermally stable photoswitchable acceptors in photochromic fluorescence resonance energy transfer (pcFRET). *J. Am. Chem. Soc.* 124:7481–7489.
15. Medintz, I., S. A. Trammell, H. Mattoussi, and J. M. Mauro. 2004. Reversible modulation of quantum dot photoluminescence using a protein-bound photochromic fluorescence resonance energy transfer acceptor. *J. Am. Chem. Soc.* 126:30–31.
16. Song, L., E. Jares-Erijman, and T. M. Jovin. 2002. A photochromic acceptor as a reversible light-driven switch in fluorescence resonance energy transfer (FRET). *J. Photochem. Photobiol. A.* 150:177–185.
17. Görner, H., and S. Matter. 2001. Photochromism of nitrospiropyrans: effects of structure, solvent and temperature. *Phys. Chem. Chem. Phys.* 3:416–423.
18. Demarco, I., A. Periasamy, C. F. Booker, and R. N. Day. 2006. Monitoring dynamic protein interactions with photoquenching FRET. *Nat. Methods.* 3:519–524.
19. Jovin, T., and D. Arndt-Jovin. 1989. Luminescence digital imaging microscopy. *Annu. Rev. Biophys. Biophys. Chem.* 18:271–308.
20. Kindermann, M., I. Sielaff, and K. Johnsson. 2004. Synthesis and characterization of bifunctional probes for the specific labeling of fusion proteins. *Bioorg. Med. Chem. Lett.* 14:2725–2728.
21. Keppler, A., H. Pick, C. Arrivoli, H. Vogel, and K. Johnsson. 2004. Labeling of fusion proteins with synthetic fluorophores in live cells. *Proc. Natl. Acad. Sci. USA.* 101:9955–9959.
22. Keppler, A., M. Kindermann, S. Gendreiziq, H. Pick, H. Vogel, and K. Johnsson. 2004. Labeling of fusion proteins of O6-alkylguanine-DNA alkyltransferase with small molecules in vivo and in vitro. *Methods.* 32:437–444.
23. Keppler, A., C. Arrivoli, L. Sironi, and J. Ellenberg. 2006. Fluorophores for live cell imaging of AGT fusion proteins across the visible spectrum. *Biotechniques.* 41:167–175.

24. Sakata, T., Y. Yan, and G. Marriott. 2005. A family of site selective optical switches. *J. Org. Chem.* 70:2009–2013.

25. Belfield, K., M. V. Bondar, C. C. Corredor, F. E. Hernandez, O. V. Przhonska, and S. Yao. 2006. Two-photon photochromism of a diarylethene enhanced by Forster resonance energy transfer from two-photon absorbing fluorenes. *Chemphyschem.* 7:2514–2519.

26. Denk, W., J. Strickler, and W. W. Webb. 1990. Two-photon laser scanning fluorescence microscopy. *Science.* 248:73–76.

27. Ando, R., H. Mizuno, and A. Miyawaki. 2004. Regulated fast nucleocytoplasmic shuttling observed by reversible protein highlighting. *Science.* 306:1370–1373.

28. Zal, T., and N. R. J. Gascoigne. 2004. Photobleaching-corrected FRET-efficiency imaging of live cells. *Biophys. J.* 86:3923–3939.

29. Chen, H., H. L. Puhl III, S. V. Koushik, S. S. Vogel, and S. R. Ikeda. 2006. Measurement of FRET efficiency and ratio of donor to acceptor concentration in living cells. *Biophys. J.* 91:L39–L41.

30. Hoppe, A., K. Christensen, and J. A. Swanson. 2002. Fluorescence resonance energy transfer-based stoichiometry in living cells. *Biophys. J.* 83:3652–3664.

31. Berney, C., and G. Danuser. 2003. FRET or no FRET: A quantitative comparison. *Biophys. J.* 84:3992–4010.

32. Mattheyses, A. L., A. D. Hoppe, and D. Axelrod. 2004. Polarized fluorescence resonance energy transfer microscopy. *Biophys. J.* 87: 2787–2797.

33. Calleja, V., D. Alcor, M. Laguerre, P. Jongsun, B. Vojnovic, B. A. Hemmings, J. Downward, P. J. Parker, and B. Larijani. 2007. Intramolecular and intermolecular interactions of protein kinase B define its activation in vivo. *PLoS Biol.* 5:780–791.

34. Jares-Erijman, E. A., L. Giordano, C. Spagnuolo, K. A. Lidke, and T. M. Jovin. 2005. Imaging quantum dots switched on and off by photochromic fluorescence resonance energy transfer (pcFRET). *Mol. Cryst. Liq. Cryst.* 430:257–265.